Crystalline Aggregates of the Repetitive Polypeptide $\{(AlaGly)_3GluGly(GlyAla)_3GluGly\}_{10}$: Structure and Dynamics Probed by ^{13}C Magic Angle Spinning Nuclear Magnetic Resonance Spectroscopy

Jianxin Wang,[†] Ajay D. Parkhe,[‡,§] David A. Tirrell,[‡] and Lynmarie K. Thompson*[,†]

Departments of Chemistry and of Polymer Science and Engineering, University of Massachusetts, Amherst, Massachusetts 01003

Received August 31, 1995; Revised Manuscript Received November 17, 1995[⊗]

ABSTRACT: A repetitive polymer comprising 10 repeats of the oligopeptide $(AlaGly)_3GluGly(GlyAla)_3GluGly$ has been synthesized via bacterial expression of an artificial gene. This polymer was designed to assemble into lamellar crystals of predictable thickness, with the oligo(AlaGly) and oligo(GlyAla) portions forming the crystal stems and the polar, bulky Glu residues lying in reverse turns between adjacent, antiparallel β-strands. The solid-state structure and dynamics of this material, before and after crystallization, have been probed with a range of magic angle spinning ^{13}C NMR experiments. Chemical shifts of backbone carbons indicate that the oligo(AlaGly) elements adopt β-conformations in all samples. Changes in both the chemical shift and cross-polarization behavior of the alanine side chains upon crystallization provide evidence for location of alanine within the crystalline β-sheet regions. In contrast, although crystallization induces changes in the chemical shift of C_α of the glutamic acid residue, no change occurs in the dynamic behavior of the Glu side chain carbons. The latter observation suggests that this side chain is excluded from the crystalline region and supports the assignment of Glu to turn positions at the lamellar surface.

Introduction

Artificial proteins prepared via microbial expression of artificial genes constitute a new class of macromolecular materials characterized by essentially absolute uniformity of chain length, sequence, and stereochemistry. The availability of such materials[1−8] has created new opportunities for design and control of the molecular and supramolecular properties of polymeric systems. Among the most intriguing possibilities is that of designing macromolecular crystals, in which crystal dimensions, chain conformation, and surface properties might be subject to precise control.

We have recently reported the biological synthesis and structural analysis of a polymer comprising 36 repeats of the octapeptide sequence **1**.[8d] Polymers of **1** were designed to adopt folded-chain lamellar architectures in the solid state, with the oligo(alanylglycine) elements forming β-strands and the periodic glutamic acid residues positioned in reverse turns at the lamellar surface. The results of spectroscopic and X-ray diffraction analyses were found to be fully consistent with the expected structure, with the β-sheet architecture confirmed via infrared, NMR, and wide-angle X-ray diffraction methods.[8d] The folding periodicity was also in accord with expectation, as shown by small-angle X-ray scattering. On the other hand, the remaining element of the design, surface confinement of the glutamic acid residues, has thus far been inferred only on the basis of indirect evidence, i.e., from the fact that ionization of the Glu side chains occurs without change in the structure or dimensions of the unit cell.[9]

The present paper concerns the structural and dynamic properties of a periodic polypeptide comprising

$$-(AG)_3EG- \quad (\mathbf{1})$$

$$-(AG)_3EG(GA)_3EG- \quad (\mathbf{2})$$

$$\{(AG)_3EG(GA)_3EG\}_{10} \quad (\mathbf{3})$$

10 repeats of the hexadecapeptide sequence **2**. This polymer is closely related to polymers of **1** but differs in that successive "β-strands" are inverted in sequence. This feature controls the registry of alanyl methyl groups in adjacent strands in any regularly folded chain conformation and has allowed us to establish that the dominant turn structures in polymers of **1** and **2** must consist of odd numbers of chain units (Figure 1). Given the widespread occurrence of three-residue (γ) turns in globular proteins, we have suggested that similar folds predominate in the crystalline periodic polypeptides examined to date.[8d,j,10] The question remains, however, to what extent the polar, bulky glutamic acid residues are localized in such folds.

Solid-state NMR spectroscopy is an important tool for the characterization of noncrystalline and semicrystalline solids and has been applied extensively to probe structure and dynamics in polymeric systems. Magic angle spinning chemical shift studies can often provide insight into structure, particularly through comparisons with model compound data. Dynamics are probed by a wide range of relaxation experiments: In polymer systems the rotating frame relaxation times, which probe kilohertz frequency motions, have proven particularly useful.[11] In this report we present solid-state NMR chemical shift, cross-polarization, and relaxation data on precipitated and crystallized preparations of a periodic polypeptide comprising 10 repeats of hexadecapeptide **2**. The data support the location of alanine side chains within the β-sheet crystalline domains and glutamyl side chains at the lamellar surfaces.

[†] Department of Chemistry.
[‡] Department of Polymer Science and Engineering.
[§] Present address: PPG Industries Inc., Chemicals Group, 440 College Park Dr., Monroeville, PA 15146.
[⊗] Abstract published in *Advance ACS Abstracts,* February 1, 1996.

0024-9297/96/2229-1548$12.00/0

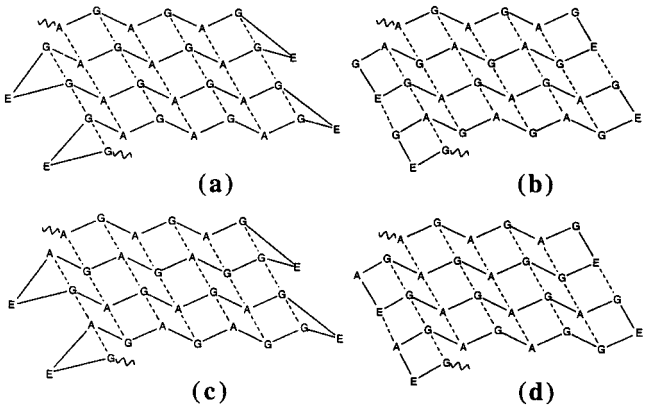

Figure 1. Schematic views of folded-chain antiparallel β-sheets of polypeptides of sequences **1** (a and b) and **2** (c and d), showing the roles of sequence and turn geometry in controlling the registry of alanyl methyl groups in adjacent strands. For **1**, the alanyl residues are in register in the structure containing three-residue folds (a) but out of register when the fold is formed by two residues (b). The situation is reversed for sequence **2** (c and d). The results of x-ray diffraction experiments are most consistent with three-residue turns in both polymers.[8d]

Experimental Section

The synthesis of polypeptide **3** was carried out in *Escherichia coli* strain BL21(DE3)pLysS under control of a bacteriophage T7 expression system.[12] The details of the polymer synthesis and purification have been outlined elsewhere.[8j] Two sample preparations, designated "precipitated" and "crystallized", respectively, were examined in this work. The precipitated sample was isolated from solution in distilled water by addition of ethanol to a final concentration of 80%. The precipitate was dried *in vacuo* at room temperature and then over P_2O_5 in a drying pistol with refluxing ethanol. The crystallized sample was prepared as follows. The polypeptide was dissolved in 90% formic acid, and the concentration of formic acid was reduced to 70% by addition of distilled water to obtain a 40 mg/mL polypeptide concentration. The solution was sheared for ca. 24 h by continuous stirring at ca. 700 rpm on a Thermix stirrer model 220T (Fisher Scientific). The formic acid concentration was reduced every 24 h by 5% by addition of water. After a few days (ca. 4 days) of continuous stirring accompanied by reduction of the formic acid concentration, a loose gel was formed. When the concentration of formic acid was 40%, i.e., after 7 days, the gel was washed three to four times in water and then three to four times with methanol. The gel was sedimented by centrifugation, and the precipitate was washed several times with water and methanol and dried over P_2O_5 in a drying pistol with refluxing ethanol.

FTIR spectra were obtained on a Nicolet IR44 bench driven by PC/IR Version 3.00 software at a resolution of 1 cm^{-1} with 50 scans/spectrum. Sample pellets were made with IR-grade KBr on a "Macro-micro KBr die" (Aldrich Chemical Co.) on a 12 ton two-column laboratory press.

Solid-state NMR spectra were obtained on a Bruker ASX 300 spectrometer with a ^{13}C NMR frequency of 75.426 MHz. The samples were typically spun at the magic angle at 5000 Hz in a solid-state probe in either a 4 or a 7 mm zirconia rotor fabricated by Bruker. All spectra were obtained using a ^{1}H NMR 90° pulse length of 5 μs, cross-polarization time of 1 ms (except for direct polarization spectra), and broad-band proton decoupling. Recycle times of 3 s for cross-polarization spectra and 15 s for direct polarization spectra were used. ^{13}C NMR spin−lattice relaxation times (T_1) were measured by the method of Torchia.[13] For ^{1}H $T_{1\rho}$ measurements, a variable length 50 kHz proton spin−lock pulse was applied between the 90° pulse and the cross-polarization pulse. For ^{13}C $T_{1\rho}$ measurements, a variable length 50 kHz carbon spin−lock pulse was applied after the cross-polarization pulse. An equivalent experiment using a 36 kHz spin−lock pulse was used to assess the contribution of spin−spin interactions to the ^{13}C $T_{1\rho}$. The above experiments were all done at room temperature. An additional measurement at ca. 260 K yielded longer ^{13}C $T_{1\rho}$values; this increase in $T_{1\rho}$ under conditions of slower motion (lower temperature) indicates that we are on the low-correlation time side of the ^{13}C $T_{1\rho}$ minimum. All spectra were calibrated using *p*-di-*tert*-butylbenzene as a standard (methyl peak at 31.0 ppm gives shift values referenced to the TMS carbon at 0 ppm). Deconvolution of NMR spectra was performed with Bruker software.

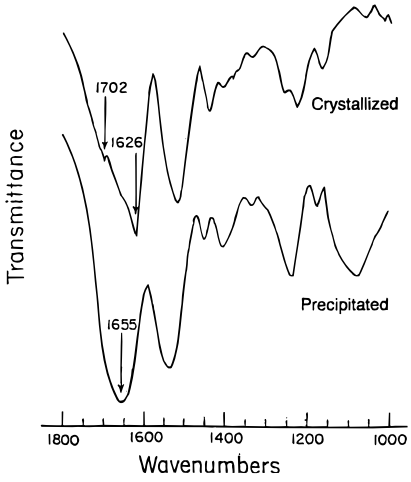

Figure 2. FTIR spectra of **3** as crystallized from formic acid (top) and as quenched from an aqueous solution by addition of ethanol (bottom).

Results and Discussion

The solid-state structure of **3** depends strongly on the method used to precipitate the polymer from its solutions in water or formic acid. Figure 2 shows infrared spectra of the two samples examined in this work. The "crystallized" sample, isolated from a sheared solution in aqueous formic acid, is characterized by amide I vibrations at 1626 and 1702 cm^{-1}, indicative of β-sheet architecture.[14,15] Precipitation from water by addition of ethanol, on the other hand, yields a relatively disordered polymer, with a broad amide I band centered at 1655 cm^{-1}.

^{13}C Chemical Shifts: Quantitation of Ordered β-Structure. The ^{13}C MAS spectra obtained with cross-polarization (CP) and with direct polarization (DP) of the precipitated and crystallized polypeptide samples are shown in Figure 3. The assignments (Table 1) are consistent with chemical shifts previously observed for β-sheet conformations of solid Ala$_n$ and Gly$_n$ polypeptides.[16,17] The Ala CO and C$_\alpha$ resonances in particular suggest that in both the precipitated and crystallized polypeptides the (AlaGly)$_3$ portion of the backbone adopts a β-conformation. However, these shifts apparently are *not* diagnostic of long-range order because ordered β-structure is observed by X-ray diffraction only *after* crystallization. Thus we will focus on the resonances that change upon crystallization as probes of the proposed β-sheet lamellar structure, which thus far has been supported by X-ray diffraction and FTIR results on the crystallized sample.

The Ala C$_\beta$ resonance demonstrates heterogeneity in the conformation of the polypeptide in both the precipitated and crystallized samples. Previous studies of related polypeptides[17] have observed chemical shifts of 19.9−21.6 ppm for the antiparallel β-sheet conformation and 14.9−17.6 ppm for various helical conformations. Thus we have assigned the 21 ppm peak, which increases upon crystallization, to the ordered β-structure

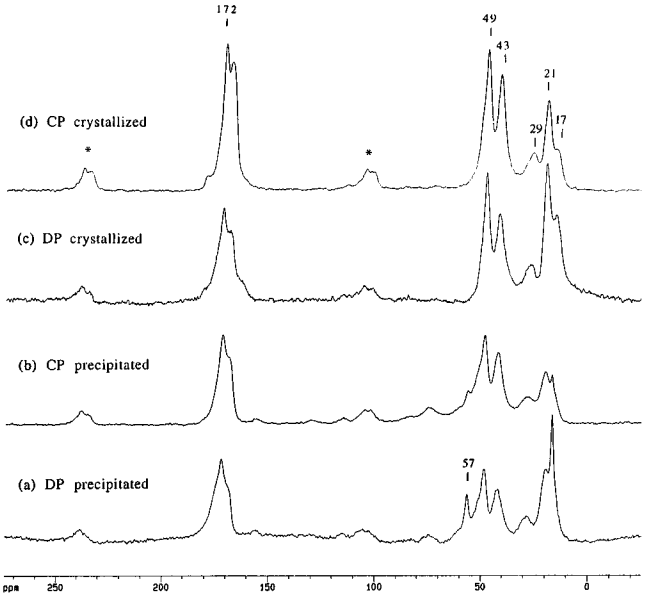

Figure 3. Solid-state magic angle spinning spectra for precipitated (a and b) and crystallized (c and d) polypeptide samples: (b and d) acquired with cross-polarization from the ^{1}H nuclei; (a and c) acquired after direct polarization of the ^{13}C nuclei. Assignments are given in Table 1; asterisk indicates spinning side bands.

Table 1. Assignment of Resonances in the Solid-State NMR Spectra

peak position (ppm)	assignment
172	alanine C═O
170	glycine C═O
57	glutamic acid C_α (disordered)
49	alanine C_α
43	glycine C_α
29	glutamic acid C_γ and C_β
21	alanine C_β (β structure)
17	alanine C_β (disordered)

and the 17 ppm peak to an alternate structure, which lacks long-range order.

The other peak that changes upon crystallization is the Glu C_α resonance, which shifts upfield from 57 ppm to ca. 49 ppm, where it is unresolved from the Ala C_α resonance. In the β-sheet conformation of Glu_n, the C_α resonance occurs at 53 ppm.[16] In general, C_α and C_β chemical shifts have been shown to be predominantly dependent on the ϕ,ψ torsion angles of the peptide backbone.[18,19] Formation of β-sheets ($-210° < \phi < -80°$ and $90° < \psi < 200°$) correlates with upfield shifts of C_α resonances; formation of α-helices ($-90° < (\phi,\psi) < -110°$) correlates with downfield shifts of C_α resonances.[18] In the proposed ordered β-sheet structure, Glu is thought to form turns (*vide supra*). The range of torsion angles previously correlated with upfield shifts is also consistent with the backbone conformations of at least two known types of turns: The central residue of an inverse γ-turn has torsion angles of $-85° < \phi < -70°$ and $60° < \psi < 70°$; and the first residue of a type II β-turn has torsion angles of $\phi = -60°$ and $\psi = 120°$.[20] Thus the upfield shift observed upon crystallization indicates a change in the conformation of the backbone at Glu, consistent with formation of a β-sheet, a type II β-turn, or an inverse γ-turn. The latter is consistent with other evidence for γ-turns in the crystallized polypeptide, as described above.

These NMR results augment the X-ray and FTIR evidence for ordered β-sheets by enabling us to estimate the amount of this structure present in each sample.

Table 2. Carbon T_1 Values for Precipitated and Crystallized Samples

	carbon T_1 (s)	
peak position (ppm)	precipitated sample	crystallized sample
172 (Ala C═O)	35.6	46.3
170 (Gly C═O)	*b*	55.5
57 (Glu C_α)	*b*	*b*
49 (Ala C_α)	16.2	17.6
43 (Gly C_α)	19.6	30.0
29[a] (Glu C_β and C_γ)	56.1 (49%), 6.0 (51%)	56.1 (30%), 6.0 (70%)
21 (Ala C_β, β)	0.61	0.40
17 (Ala C_β, other)	0.76	*b*

[a] The intensity data were fit to a biexponential decay, $I_1 \exp(-t/T_{1_1}) + I_2 \exp(-t/T_{1_2})$; the two relative intensities and relaxation times are reported. [b] These peaks were too weak in the CP MAS spectra for T_1 measurements.

Peak intensities are compared in the direct polarization spectra in order to avoid errors due to differences in cross-polarization efficiencies for different types of carbons. Furthermore, such intensities are accurate only if experimental parameters allow sufficient time for complete relaxation of the ^{13}C resonance. The ^{13}C T_1 values (Table 2) indicate that the direct polarization experiment, performed with a 15 s repetition rate, will give accurate intensities for the rapidly relaxing Ala C_β (both forms), which is the only resonance that is clearly resolved for the two structural forms. The relative areas of the 17 and 21 ppm peaks were measured by deconvolution of the DP spectra: In the precipitated polypeptide about 28% of alanine β-carbons are in the ordered β-structure; in the crystallized sample about 64% of alanine β-carbons are in the ordered β-structure (21 ppm peak). Thus both samples can be described as partially ordered. The ability to measure the extent of formation of ordered β-structure with NMR may be quite useful for optimization of crystallization conditions for these materials.

^{1}H $T_{1\rho}$ Indicates Materials Are Uniform on the Nanometer Scale. Proton $T_{1\rho}$ measurements can be used to probe for inhomogeneities in polymeric solids.[21] If domains within the sample are small, rapid ^{1}H NMR spin diffusion leads to a single value for the ^{1}H $T_{1\rho}$ measured via each carbon. However, the presence of large domains with distinct relaxation times can lead to the observation of multiple $T_{1\rho}$ values—either distinct relaxation times are observed for resonances associated with distinct domains or biexponential behavior is observed for an unresolved resonance. The polypeptide samples examined herein show no evidence of such heterogeneity: a single ^{1}H $T_{1\rho}$ is measured for all carbons in each sample (5.9 ± 0.4 ms in the precipitated sample and 8.2 ± 0.3 ms in the crystallized sample, Table 3). Thus the conversion of about 40% of the sample from a disordered to an ordered β-structure increases the proton $T_{1\rho}$ measurably, suggesting that the two structural phases have distinct intrinsic $T_{1\rho}$ values and that the presence of distinct domains could be detected by this method. The measured values for $T_{1\rho}$ (6−8 ms) place an upper limit of about 2−3 nm on the size of domains present in the samples.[21] This domain size indicates that the disordered portions of both samples are interspersed with the ordered β-structure such that protons in the ordered phase are not more than 30 Å from the protons in the disordered phase (insuring rapid equilibration by spin diffusion). This is in reasonable agreement with the expected chain−axis dimension of the ordered phase: Turns at every Glu residue give a stem length of about 30 Å, and the

Table 3. Proton $T_{1\rho}$ Values for Precipitated and Crystallized Samples

	proton $T_{1\rho}$ (ms)[a]	
peak position (ppm)	precipitated sample	crystallized sample
172 (Ala C=O)	5.8	7.8
170 (Gly C=O)	*b*	7.9
57 (Glu C_α)	6.1	*b*
49 (Ala C_α)	5.8	8.5
43 (Gly C_α)	6.5	8.4
29 (Glu C_β & C_γ)	6.0	8.0
21 (Ala C_β, β)	6.3	8.8
17 (Ala C_β, other)	5.1	8.0
average	5.9 ± 0.4	8.2 ± 0.3

[a] The intensity data were fit to the form $I \exp(-t/T_{1\rho})$, where t is the spin−lock time. [b] These peaks were too weak in the CP MAS spectra for $T_{1\rho}$ measurements.

Table 4. Carbon $T_{1\rho}$ Values for Precipitated and Crystallized Samples

	average carbon $T_{1\rho}$ (ms)[a]	
peak position (ppm)	precipitated sample	crystallized sample
172 (Ala C=O)	30	29
170 (Gly C=O)	*b*	20
57 (Glu C_α)	4.3	*b*
49 (Ala C_α)	14	21
43 (Gly C_α)	12	11
29 (Glu C_β & C_γ)	3.8	3.9
21 (Ala C_β, β)	16	23
17 (Ala C_β, other)	16	12

[a] The data for spin-lock times of 60 μs to 20 ms were fit to a biexponential decay, $I_1 \exp(-t/T_{1_1}) + I_2 \exp(-t/T_{1_2})$, and the average carbon $T_{1\rho} = \left[\frac{I_1}{T_{1_1}} + \frac{I_2}{T_{1_2}}\right]^{-1}$ is reported. [b] These peaks were too weak in the CP MAS spectra for $T_{1\rho}$ measurements.

related polymers of **1** are known to be characterized by similar lamellar thicknesses.[8d] The other two crystal dimensions are not defined by the chain sequence and are likely to depend on crystallization conditions.

The single relaxation rate observed in both samples is the weighted average of the relaxation rates of the two structural phases of the polypeptide, disordered and ordered β-sheet. Thus the relaxation rates for the pure forms can be calculated from the observed rates for the two compositions, which yields estimated $T_{1\rho}$ values of about 14 ms for the ordered β-structure and 5 ms for the disordered structure. On the other hand, these estimates would not be valid if the crystallization protocol itself alters the relaxation rates of one or both phases of the polypeptide. In either case, the observed increase in the proton $T_{1\rho}$ value upon crystallization indicates there is a decrease in molecular motions at the 50 kHz rate probed by this experiment, consistent with a general decrease in mobility expected upon crystallization. More specific information about mobilities of different groups on several time scales is provided by the carbon cross-polarization and relaxation experiments presented below.

Cross-Polarization Dynamics: Evidence for Stacking Interactions between β-Sheets. Comparison of the spectra (Figure 3) obtained with CP and with DP indicates that the two carbons that change their chemical shift upon crystallization, as described above, also are different in their dynamic behavior from the other carbons in the sample. Both Ala C_β and Glu C_α show the most significant differences in intensity between the CP and DP spectra; particularly in the precipitated sample, the 17 and 57 ppm peaks are substantially enhanced in the DP spectra. This indicates that these carbons are not cross-polarizing efficiently, presumably because rapid motion in the disordered structure is averaging the CH dipolar interactions needed for efficient cross-polarization. Such motion must be of sufficiently large amplitude to achieve isotropic averaging of the dipolar interaction. For instance, C_3 rotation of a methyl group is insufficient, for it leaves a net CH dipolar coupling; reorientation of the entire methyl group is needed for isotropic averaging. Thus it appears that in the disordered portions of the sample, both the Ala methyl and the Glu C_α are undergoing such large amplitude motions. The low ^{13}C T_1 values of the Ala methyl (Table 2) indicate that methyl group motion is also occurring on the 10^{-8} s time scale (presumably C_3 rotation; see below). In the ordered β-structure (21 ppm peak), T_1 is unchanged but cross-polarization is more efficient: The methyl rotation is unaltered, but the large amplitude motion is prevented. This is consistent with the Ala methyl group residing within the ordered β-sheet structure, with its motion constrained by intersheet packing. The high mobility of the Glu C_α peak in the precipitated polypeptide (57 ppm peak) may indicate this charged residue resides in large pockets without interstrand backbone hydrogen bonding. Unfortunately the lack of resolution of this peak after crystallization makes it impossible to deduce whether this mobility changes for Glu C_α in the ordered β-sheet structure.

Relaxation Behavior Provides Further Support for the Structural Model. Relaxation rates are enhanced by motions which produce dipolar fluctuations with frequencies that match the transition. Thus carbon laboratory-frame spin−lattice relaxation rates are enhanced (and relaxation times minimized) by motion with correlation times on the 10^{-8} s time scale (the T_1 minimum is expected when $1/\tau_c = \omega_{Larmor} = 75$ MHz). Lower frequency (kilohertz) motions can be probed through measurements of the rotating-frame spin−lattice relaxation time, $T_{1\rho}$, by spin−locking the magnetization with a pulse producing a lower (arbitrary) field strength. Thus the carbon and proton rotating-frame spin−lattice relaxation rates are enhanced (and relaxation times minimized) by motion with correlation times on the 10^{-5} s time scale (the $T_{1\rho}$ minimum is expected when $1/\tau_c = \omega_{spin-lock} = 50$ kHz).

The measured carbon T_1 values (Table 2) are quite similar to those reported by Saito for silk and solid Ala$_n$.[22] Only the Ala methyl group has a short T_1, indicating that it undergoes C_3 rotation on the 10^{-8} time scale and that the backbone is immobile on this time scale. Relaxation of other carbons is dominated by dipolar contributions from directly bound protons (thus the CO relaxation is slower than C_α) and the rotating methyl group. Because the latter contribution drops off sharply with distance, the Ala C_α and CO relax faster than the Gly C_α and CO, respectively, as was also observed in silk.[22] It is not surprising that crystallization does not alter these relaxation times significantly: Since the backbone experiences little motion on this time scale, T_1 is not a sensitive detector of motional changes. The rapid rotation of the methyl group is apparently unimpeded by crystal packing.

^{13}C $T_{1\rho}$ measurements were performed in order to probe lower frequency motions of the polypeptide. Data obtained with spin-lock times between 60 μs and 20 ms were fit to a biexponential decay; the weighted average of the resulting $T_{1\rho}$ values is reported in Table 4. Similar trends and conclusions result from single exponential fits to the full data set or the initial (≤2 ms)

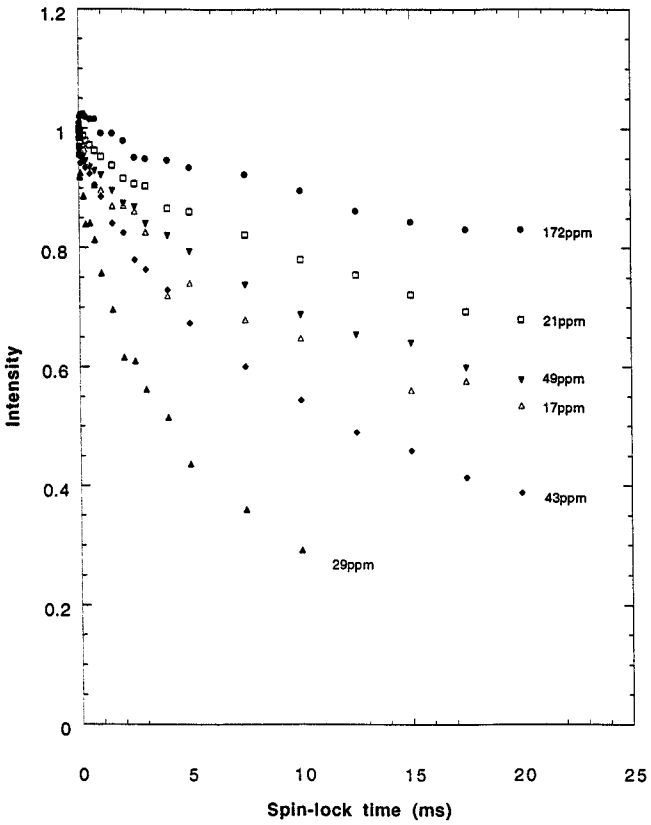

Figure 4. ^{13}C NMR rotating frame relaxation time ($T_{1\rho}$) for the crystallized polypeptide. The normalized intensity of the resonances is plotted against the variable spin-lock time: carbonyl carbon at 172 ppm, ●; alanine α-carbon at 49 ppm, ▼; glycine α-carbon at 43 ppm, ◆; alanine β-carbon at 21 ppm, □; alanine β-carbon at 17 ppm, Δ; glutamic acid β- and γ-carbons at 29 ppm, ▲.

data; Figure 4 shows the full data set for the crystallized polypeptide. The Ala and Gly backbone resonances have medium to long relaxation times of 11−30 ms (shortest for Gly C_α with its two bound protons). Upon crystallization there are again only small changes in the backbone relaxation times, suggesting there is little change in kilohertz motions for the Ala and Gly backbone carbons in the sample. This suggests that the backbone mobility is similarly restricted by interstrand hydrogen bonding in both the disordered and ordered structures. Interestingly, the Ala side chain carbon also relaxes on this medium time scale (12−23 ms) similar to the backbone: The methyl group rotation which shortens its ^{13}C T_1 does not have major components in the 50 kHz range needed to substantially enhance the ^{13}C $T_{1\rho}$. There is a small increase in relaxation time upon formation of β-structure (21 ppm peak), consistent with some reduction in mobility of the methyl group due to intersheet packing interactions.

The Glu backbone C_α peak (57 ppm) and side chain C_β and C_γ peaks (unresolved at 29 ppm) have the most rapid ^{13}C $T_{1\rho}$ relaxation in the sample (4 ms), suggesting that the motion of this residue has components in the kilohertz frequency range. This is consistent with the inefficient CP results which suggested that Glu residues in the disordered structure reside in pockets without interstrand hydrogen bonding. However the relaxation of the side chain and thus its mobility appear unchanged upon formation of ordered β-structure. If the side chain were to be found within the ordered β-structure, it should have its motion substantially restricted by packing interactions. On the other hand, if the Glu residues form the turns as proposed, the side chain should have significant motional freedom in its location on the lamellar surfaces. Thus the lack of change in the ^{13}C $T_{1\rho}$ which probes the kilohertz range motions of the Glu side chain supports its proposed location at the turns of the ordered stacks of β-sheets.

One pitfall in using such measurements to probe motion is that ^{13}C $T_{1\rho}$ values can also be shortened by $^1H-^{13}C$ spin−spin interactions. Although the contribution of spin−spin interactions to $T_{1\rho}$ can be measured quantitatively,[23] the following qualitative arguments suggest that it is not dominant in these experiments. Domination of ^{13}C $T_{1\rho}$ by spin−spin interactions has typically been observed in rigid crystalline samples such as glycine,[23] unlike these samples which are only partially crystalline. The extent to which the ^{13}C $T_{1\rho}$ values are shortened by spin−spin interactions should vary with the extent of crystallinity: If the crystallized sample were sufficiently rigid that spin−spin interactions shorten $T_{1\rho}$, this effect should be less significant in the precipitated sample, leading to longer $T_{1\rho}$ values. However, the $T_{1\rho}$ values do not decrease substantially upon crystallization. The $T_{1\rho}$ values are approximately proportional to the square of the spin−lock field strength (data not shown) as expected for a spin−lattice $T_{1\rho}$; a much stronger field dependence is typically observed in cases where $T_{1\rho}$ is dominated by spin−spin interactions.[11,23] Thus ^{13}C $T_{1\rho}$ values are likely to be good probes of dynamics in these materials. The short Glu side chain ^{13}C $T_{1\rho}$ values indicate that these carbons undergo significant 50 kHz range motions; the lack of change in these rapid motions upon crystallization suggests this side chain resides in an unconstrained (noncrystalline) environment in both cases, consistent with its proposed location at the surfaces of the crystals.

Conclusions

The chemical shift, cross-polarization, and relaxation data presented above provide a useful picture of the structure and dynamics of polymeric solids prepared from repetitive polypeptides of sequence **2**. Both the precipitated and crystallized samples are partially ordered and uniform on the nanometer scale (based on a single ^1H $T_{1\rho}$). The fraction of ordered β-structure can be determined by the Ala C_β resonances. There is a decrease in overall mobility (50 kHz regime) upon crystallization, reflected in an increase in the ^1H $T_{1\rho}$.

The oligo(alanylglycine) (and oligo(glycylalanine)) portions of the backbone appear to be in a β-strand conformation with interstrand hydrogen bonding in both the disordered and ordered materials, based on their chemical shifts and the lack of change in chemical shifts and dynamics upon crystallization. The Ala side chain clearly changes both its electronic environment and dynamics upon crystallization: Both its 21 ppm chemical shift and the loss of its large-amplitude motions (increasing its CP efficiency) indicate that it resides in an ordered β-structure in the crystallized sample. Thus the stem regions of the polypeptide appear to change from loosely packed β-strands characterized by significant isotropic Ala side chain motions to stacks of β-sheets, which lock out large-amplitude methyl motions.

The backbone differs at the Glu residues (C_α) in that (1) it is more mobile (inefficient CP and short ^{13}C $T_{1\rho}$) than the AlaGly portions in the disordered structure and (2) it changes its electronic environment (chemical shift) substantially upon crystallization. The Glu side chains

(C_β and C_γ) are also unique in having a short ^{13}C $T_{1\rho}$, which is retained upon crystallization. The dynamic behavior of the backbone and side chain suggests that in the disordered structure the bulky Glu residues may reside in pockets and lack interstrand hydrogen bonding. The chemical shift change upon crystallization indicates a change in backbone conformation, which is consistent with formation of β- or turn structures. However the retention of a highly dynamic side chain makes the β-structure seem unlikely: There would be insufficient space for the bulky Glu side chain without disrupting the packing needed to prevent the Ala methyl group motions as described above. On the other hand, the formation of turns at the Glu residues would allow the bulky side chain to retain its dynamic behavior, for it would be free of crystalline packing constraints at the surface of the lamellar material.

Acknowledgment. This research was supported by grants from the NSF Materials Science and Engineering Center at the University of Massachusetts, an award from Research Corporation (L.K.T.), and an NSF Young Investigator Award (L.K.T.). The NMR instrument was purchased with a grant from NSF (BIR-911996) and matching funds from the University of Massachusetts. The authors acknowledge Drs. Charles Dickinson and Alan Waddon for helpful discussions.

References and Notes

(1) Cappello, J.; Ferrari, F. In *Plastics from Microbes: Microbial Synthesis of Polymers and Polymer Precursors*; Mobley, D. P., Ed.; Hanser/Gardner Publications: Munich, 1994; p 35.
(2) Case, S. T.; Powers, J.; Hamilton, R.; Burton, M. J. In *Silk Polymers;* Kaplan, D., Adams, W. W., Farmer, B., Viney, C., Eds.; ACS Symposium Series 544; American Chemical Society: Washington, DC, 1994; p 81.
(3) Goldberg, I.; Salerno, A. J. In *Materials Synthesis Utilizing Biological Processes*; Reike, P. C., Calvert, P. D., Alper, M., Eds.; Materials Research Society Proceedings 174; Materials Research Society: Pittsburgh, PA, 1990; p 229.
(4) McPherson, D. T.; Morrow, C.; Minehan, D. S.; Wu, J.; Hunter, E.; Urry, D. W. *Biotechnol. Prog.* **1992**, *8*, 347.
(5) Salerno, A. J.; Goldberg, I. *Appl. Microbiol. Biotechnol.* **1993**, *58*, 209.
(6) O'Brien, J. P.; Hoess, R. H.; Gardner, K. H.; Lock, R. L.; Wasserman, Z. R.; Weber, P. C.; Salemme, F. R. In *Silk Polymers*; Kaplan, D., Adams, W. W., Farmer, B., Viney, C., Eds.; ACS Symposium Series 544; American Chemical Society: Washington, DC, 1994; p 104.
(7) McGrath, K. P.; Kaplan, D. L. In *Biomolecular Materials*; Viney, C.; Case, S. T., Waite, J. H., Eds.; Materials Research Society Proceedings 292; Materials Research Society: Pittsburg, PA, 1993; p 83.
(8) (a) McGrath, K. P.; Fournier, M. J.; Mason, T. L.; Tirrell, D. A. *J. Am. Chem. Soc.* **1992**, *114*, 727. (b) Creel, H. S.; Fournier, M. J.; Mason, T. L.; Tirrell, D. A. *Macromolecules* **1991**, *24*, 1213. (c) Zhang, G.; Fournier, M. J.; Mason, T. L.; Tirrell, D. A. *Macromolecules* **1992**, *25*, 3601. (d) Krejchi, M. T.; Atkins, E. D. T.; Waddon, A. J.; Fournier, M. J.; Mason, T. L.; Tirrell, D. A. *Science* **1994**, *265*, 1427. (e) Beavis, R. C.; Chait, B. T.; Creel, H. S.; Fournier, M. J.; Mason, T. L.; Tirrell, D. A. *J. Am. Chem. Soc.* **1992**, *114*, 7584. (f) Yoshikawa, E.; Fournier, M. J.; Mason, T. L.; Tirrell, D. A. *Macromolecules* **1994**, *27*, 5471. (g) Kothakota, S.; Mason, T. L.; Fournier, M. J.; Tirrell, D. A. *J. Am. Chem. Soc.* **1995**, *117*, 536. (h) Deguchi, Y.; Fournier, M. J.; Mason, T. L.; Tirrell, D. A. *J. Macromol. Sci. Pure Appl. Chem.* **1994**, *A31*, 1691. (i) Dougherty, M. J.; Kothakota, S.; Mason, T. L.; Tirrell, D. A.; Fournier, M. J. *Macromolecules* **1993**, *26*, 1779. (j) Parkhe, A.; Fournier, M. J.; Mason, T. L.; Tirrell, D. A. *Macromolecules* **1993**, *26*, 6691.
(9) Chen, C. C.; Krejchi, M. T.; Hsu, S. L.; Tirrell, D. A. *Macromolecules* **1995**, *28*, 1464.
(10) Y. Deguchi, M. T. Krejchi, M. J. Fournier, D. A. Tirrell, S. Cooper, and E. D. T. Atkins, submitted for publication.
(11) Schaefer, J.; Stejskal, E. O.; Buchdahl, R. *Macromolecules* **1977**, *10*, 384.
(12) Rosenburg, A. H.; Lade, B. N.; Chui, D.; Lin, S.; Dunn, J. J.; Studier, F. W. *Gene* **1987**, *56*, 125.
(13) Torchia, D. A. *J. Magn. Reson.* **1978**, *30*, 613.
(14) Bandekar, J.; Krimm, S. In *Advances in Protein Chemistry;* Anfinsen, C. B., Edsall, J. T., Richards, F. M., Eds.; Academic Press: Orlando, FL, 1986; Vol. 38, p 183.
(15) Krimm, S.; Abe, Y. *Proc. Natl. Acad. Sci. U.S.A.* **1972**, *69* (10) , 2788.
(16) Kricheldorf, H. R.; Müller, D. *Macromolecules* **1983**, *16*, 615.
(17) Saito, H.; Tabeta, R.; Asakura, T.; Iwanaga, Y.; Shoji, A.; Ozaki, T.; Ando, I. *Macromolecules* **1984**, *17*, 1405.
(18) Spera, S.; Bax, A. *J. Am. Chem. Soc.* **1991**, *113*, 5490.
(19) de Dios, A. C.; Pearson, J. G.; Oldfield, E. *Science* **1993**, *260*, 1491.
(20) Creighton, T. E. *Proteins*: *Structures and Molecular Properties*; W. H. Freeman & Co: New York, 1993; p 226.
(21) Dickinson, L. C.; Yang, H.; Chu, C. W.; Stein, R. S.; Chien, J. C. W. *Macromolecules* **1987**, *20*, 1757.
(22) Saito, H.; Ishida, M.; Yokoi, M.; Asakura, T. *Macromolecules* **1990**, *23*, 83.
(23) Schaefer, J.; Sefcik, M. D.; Stejskal, E. O.; McKay, R. A. *Macromolecules* **1984**, *17*, 1118.

MA9512972